OBSERVE-BASED DIRECT YAW-MOMENT H∞ CONTROL FOR IN-WHEEL-MOTORED ELECTRIC VEHICLE

[1]ZHIYONG ZHANG, [2]ZHIQIANG LIU, [3]XIN LIU, [4]CAIXIA HUANG

[1,3]Dr., College of Automotive and Mechanical Engineering, Changsha University of Science and
Technology, Changsha 410004, PR China
[2]Assoc. Prof., College of Automotive and Mechanical Engineering, Changsha University of Science and
Technology, Changsha 410004, PR China
[4]Dr., College of Mechanical vehicle Engineering, Hunan university, Changsha 410082, PR China
E-mail: [1]zzy04@163.com , [2] lzq0228@126.com , [3] lxym810205@163.com , [4] huangcaixia@hnu.edu.cn

ABSTRACT

This paper presented a new method for four wheel in-wheel-motored electric vehicle to improve handling and stability with the help of sideslip angle observer and braking force distribution. The first part of this study deals with the full description of the basic theory of vehicle dynamic control system. After that four wheels in-wheel-motored electric vehicle dynamics model, as well as desired dynamic response model were built. Furthermore, direct yaw-moment control (DYC) system, as well as sideslip angle observer and braking force distribution, were also presented. Therein, an observe-based direct yaw-moment H∞ feedback control loop was employed to track the desired dynamic response via braking force distribution between four in-wheel motors. Finally, the open-loop and closed-loop simulation for validation were performed. The results verified that, the proposed vehicle dynamic control system can improve vehicle handling and stability significantly.

Keywords: *Electric Vehicle, Four Wheel Drive, In-Wheel Motor, Direct Yaw-moment Control (DYC), Braking Force Distribution*

1. INTRODUCTION

With the increase in interest and demand in vehicle safety, active safety technology has become very important and has motivated extensive research activities. For a road vehicle, many severe accidents result from the loss of stability directly or indirectly, which may be attributed to emergency steering or μ-split braking due to different road surface adhesion. Vehicle stability control systems are designed to enhance vehicle stability by correcting the motion attitude via active steering [1] or direct yaw moment adjustment [2]. Such vehicle dynamics and stability enhancement systems are called vehicle dynamics controller (VDC) or electronic stability program (ESP). Most commercially available VDC systems use the latter method involving individual wheel braking action, because it is more easily accomplished using already existing hardware.

Meanwhile, in order to conserve energy and protect the environment, the development of new generation electric vehicle have become a hotspot in automotive research and development [3]. Because the four wheel in-wheel-motored electric

vehicle canceled the traditional power train, they have advantage of packing flexibility, space-saving, high mechanical efficiency and have been recognized as a break-through concept that will have a major impact on future electric and hybrid vehicle design [4]. Another advantage of four wheel in-wheel-motored electric vehicle is they can distribute different driving/braking force on four wheels to enhance vehicle maneuverability and lateral stability. Unfortunately, lots of related researches focus on the direct yaw-moment calculation which based on the error between actual yaw rate and side slip angle and reference values. In some cases, however, how to realize the direct yaw-moment by the braking forces of four wheels is absolutely critical because there are tire adhesion limits. This paper not only describes a VDC algorithm for four wheels in-wheel-motored electric vehicle to improve vehicle maneuverability and lateral stability, but also proposes a strategy of braking force distribution based on linear programming.

2. VEHICLE DYNAMICS

A vehicle model in planar motion is shown in Figure 1. Considering only the planar motion, the

external forces act on vehicle are the lateral forces and longitudinal forces on four wheels, which cause the lateral motion and the yaw motion of the vehicle. The governing equations of the lateral and the yaw motion can be expressed as follows:

$$mV\left(\dot{\beta}+\gamma\right)=F_{y1}+F_{y2}+F_{y3}+F_{y4} \tag{1}$$

$$I_z\dot{\gamma}=l_f\left(F_{y1}+F_{y2}\right)-l_r\left(F_{y3}+F_{y4}\right)+M_z \tag{2}$$

where, $M_z=0.5t_w\left(F_{x1}-F_{x2}+F_{x3}-F_{x4}\right)$ is the direct yaw-moment that generated by driving/braking forces on four wheels; m is the vehicle mass; V is the vehicle velocity; β is the vehicle sideslip angle, which is defined as $\beta=\arctan(V_y/V_x)$; γ is the yaw rate; I_z is the moment of inertia about Z axis; $F_{xi}(i=1,2,3,4)$ and $F_{yi}(i=1,2,3,4)$ are the longitudinal and lateral forces of the i-th wheel, respectively; l_f and l_r are the distance from vehicle center of gravity to front and rear axle, respectively.
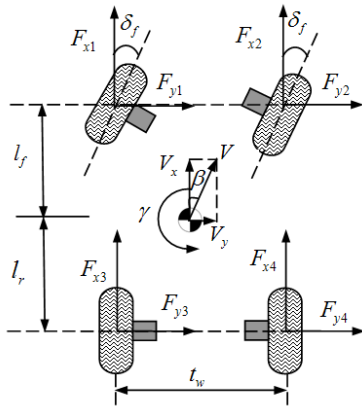

Figure 1: Planar Motion Vehicle Model

Because γ is small, the lateral forces of four wheels can be expressed as following:

$$\begin{aligned}F_{y1}&=F_{y2}=C_f\left(\delta_f-\beta-l_f\gamma/V_x\right)\\F_{y3}&=F_{y4}=C_r\left(-\beta+l_r\gamma/V_x\right)\end{aligned} \tag{3}$$

The state space model of 2-DOF vehicle model can be rewritten as:

$$\dot{\tilde{x}}=\tilde{A}x+\tilde{B}_1w+\tilde{B}_2u \tag{4}$$

where, $\tilde{x}=\begin{bmatrix}\beta & \gamma\end{bmatrix}^T$, $\tilde{w}=\begin{bmatrix}\delta_f\end{bmatrix}$, $\tilde{u}=\begin{bmatrix}M\end{bmatrix}$,

$$\tilde{A}=\begin{bmatrix}-\dfrac{2C_r+2C_f}{m_tV_x} & \dfrac{2C_rl_r-2C_fl_f}{m_tV_x^2}-1\\ \dfrac{2C_rl_r-2C_fl_f}{I_z} & -\dfrac{2C_rl_r^2+2C_fl_f^2}{I_zV_x}\end{bmatrix},$$

$$\tilde{B}_1=\begin{bmatrix}\dfrac{2C_f}{m_tV_x}\\ \dfrac{2C_fl_f}{I_z}\end{bmatrix},\quad \tilde{B}_2=\begin{bmatrix}0\\ \dfrac{1}{I_z}\end{bmatrix}.$$

3. VEHICLE DYNAMIC CONTROL SYSTEM

3.1 Desired Dynamic Response Model

For the yaw rate response reflects the handling performance and the slip response reflects stability performance, they are often regarded as desired responses and tracked by actual vehicle. Generally, the desired side slip angle of vehicle is equal to zero [5].

$$\beta_d=0 \tag{5}$$

The desired yaw rate response can be calculated based on the vehicle steering angle and longitudinal velocity. In this paper, a first order yaw rate response model is selected and the desired yaw rate response can be described as [6]:

$$\gamma_d=k_\gamma\delta_f/\left(1+\tau_\gamma s\right) \tag{6}$$

where, $\tau_\gamma=\dfrac{I_zV_x}{2C_fl_f\left(l_f+l_r\right)+m_tl_rV_x^2}$,

$$k_\gamma=\dfrac{V_x}{l_f+m_tl_fl_rV_x^2\Big/2C_fl_f\left(l_f+l_r\right)^2}.$$

The desired model, Equations (5) and (6), can be expressed in state space form as follows:

$$\dot{x}_d=A_dx_d+B_d\tilde{w} \tag{7}$$

Where, $x_d=\begin{bmatrix}\beta_d\\ \gamma_d\end{bmatrix}$, $A_d=\begin{bmatrix}0 & 0\\ 0 & -\dfrac{1}{\tau_\gamma}\end{bmatrix}$, $B_d=\begin{bmatrix}0\\ k_\gamma/\tau_\gamma\end{bmatrix}$.

The Equation (6) assumes the road adhesion coefficient is sufficiently high and can afford enough lateral force in any circumstance. But there is upper bound for wheel force and the lateral acceleration of the vehicle cannot exceed the maximum friction coefficient. So the limit of desired yaw rate can be expressed by following value [7]:

$$\left|\dot{\psi}_d\right|=\left|\mu g/V_x\right| \tag{8}$$

We define an error vector about yaw rate and side slip angle as follow:

$$x=\tilde{x}-x_d=\begin{bmatrix}\beta-\beta_d\\ \dot{\psi}-\dot{\psi}_d\end{bmatrix} \tag{9}$$

So the state space form of 2-DOF vehicle model with error vector can be written as:

$$\dot{x} = \tilde{A}x + \left(\tilde{B}_1 - B_d\right)\tilde{w} + \tilde{B}_2\tilde{u} + \left(\tilde{A} - A_d\right)x_d$$

$$= \tilde{A}x + \left[\tilde{A} - A_d \quad \tilde{B}_1 - B_d\right]\begin{bmatrix} x_d \\ \tilde{w} \end{bmatrix} + \tilde{B}_2\tilde{u} \quad (10)$$

$$= Ax + B_1 w + B_2 u$$

where, $A = \tilde{A}$, $B_2 = \tilde{B}_2$, $w = \begin{bmatrix} \beta_d & \gamma_d & \delta_f \end{bmatrix}^T$, $u = \tilde{u}$,

$$B_1 = \begin{bmatrix} -\dfrac{2C_r + 2C_f}{m_t V_x} & \dfrac{2C_r l_r - 2C_f l_f}{m_t V_x^2} - 1 & \dfrac{2C_f}{m_t V_x} \\ \dfrac{2C_r l_r - 2C_f l_f}{I_z} & -\dfrac{2C_r l_r^2 + 2C_f l_f^2}{I_z V_x} + \dfrac{1}{\tau_\gamma} & \dfrac{2C_f l_f}{I_z} - \dfrac{k_\gamma}{\tau_\gamma} \end{bmatrix}.$$

3.2 Sideslip Observer

Because the yaw rate can be measured directly by sensor, the error of yaw rate between the actual response and the desired response is defined as measured output. In vehicle dynamics response, the yaw rate reflects more handling performance and slide slip angle reflects more stability performance, so the errors of the yaw rate and the side slip angle are selected as regulated output that should be minimized by controller. The equations of 2-DOF vehicle dynamics, regulated output and measured output are unified as following:

$$\begin{cases} \dot{x}(t) = Ax(t) + B_1 w(t) + B_2 u(t) \\ z(t) = C_1 x(t) + D_1 w(t) \\ y(t) = C_2 x(t) + D_2 u(t) \end{cases} \quad (11)$$

where, $z(t)$ is regulated output and $y(t)$ is measured output. The matrices in them are defined as: $C_1 = \begin{bmatrix} 1 & 0 \\ 0 & 1 \end{bmatrix}$, $D_1 = \begin{bmatrix} 0 & 0 & 0 \\ 0 & 0 & 0 \end{bmatrix}$, $C_2 = \begin{bmatrix} 0 & 1 \end{bmatrix}$, $D_2 = \begin{bmatrix} 0 \end{bmatrix}$.

Since the sideslip angle is difficult to measure directly by sensor, the following modified observer-based control is proposed to estimate the side slip angle and stabilize the system (11).

$$\begin{cases} \dot{\hat{x}}(t) = A_c \hat{x}(t) + B_2 u(t) + L\left(y(t) - \hat{y}(t)\right) \\ \hat{y}(t) = C_2 \hat{x}(t) + D_2 u(t) \\ u(t) = K\hat{x}(t) \end{cases} \quad (12)$$

where, $\hat{x}$ is the estimation of x, L is the observer gain, $\hat{y}$ is the observer output, K is the controller gain. The matrices A_c, L and K are determined by LMIs optimization.

3.3 The Optimal H_∞ Controller

Defined $e(t) = x(t) - \hat{x}(t)$ as the estimated state error, the Equations (11) and (12) can be expressed as:

$$\begin{bmatrix} \dot{\hat{x}}(t) \\ \dot{e}(t) \end{bmatrix} = \begin{bmatrix} A_c + B_2 K & LC_2 \\ A - A_c & A - LC_2 \end{bmatrix}\begin{bmatrix} \hat{x}(t) \\ e(t) \end{bmatrix} + \begin{bmatrix} 0 \\ B_1 \end{bmatrix} w(t)$$
(13)

Here define a Lyapunov equation as:

$$V\left(\hat{x}(t), e(t)\right) = \hat{x}^\mathrm{T}(t)P_1\hat{x}(t) + e^\mathrm{T}(t)P_2 e(t) \quad (14)$$

where, $P_1 > 0$ and $P_2 > 0$.

The time derivative of $V\left(\hat{x}(t), e(t)\right)$ alone the trajectories of (14) is:

$$\dot{V}\left(\hat{x}(t), e(t)\right) = \begin{bmatrix} \hat{x}(t) \\ e(t) \end{bmatrix}^T \begin{bmatrix} A_c^T + K^T B_2^T & A^T - A_c^T \\ C_2^T L^T & A^T - C_2^T L^T \end{bmatrix}\begin{bmatrix} P_1 & 0 \\ 0 & P_2 \end{bmatrix}\begin{bmatrix} \hat{x}(t) \\ e(t) \end{bmatrix}$$

$$+ \begin{bmatrix} \hat{x}(t) \\ e(t) \end{bmatrix}^T \begin{bmatrix} P_1 & 0 \\ 0 & P_2 \end{bmatrix}\begin{bmatrix} A_c + B_2 K & LC_2 \\ A - A_c & A - LC_2 \end{bmatrix}\begin{bmatrix} \hat{x}(t) \\ e(t) \end{bmatrix}$$

$$+ w^T(t)\begin{bmatrix} 0 & B_1^T \end{bmatrix}\begin{bmatrix} P_1 & 0 \\ 0 & P_2 \end{bmatrix}\begin{bmatrix} \hat{x}(t) \\ e(t) \end{bmatrix} + \begin{bmatrix} \hat{x}(t) \\ e(t) \end{bmatrix}^T\begin{bmatrix} P_1 & 0 \\ 0 & P_2 \end{bmatrix}\begin{bmatrix} 0 \\ B_1 \end{bmatrix}w(t)$$

$$= \begin{bmatrix} \hat{x}(t) \\ e(t) \\ w(t) \end{bmatrix}^T \begin{bmatrix} \Sigma_1 & \Sigma_2 & 0 \\ \Sigma_2^T & \Sigma_3 & P_2 B_1 \\ 0 & B_1^T P_2 & 0 \end{bmatrix}\begin{bmatrix} \hat{x}(t) \\ e(t) \\ w(t) \end{bmatrix}$$
(15)

where, $\Sigma_1 = A_c^T P_1 + K^T B_2^T P_1 + P_1 A_c + P_1 B_2 K$,

$\Sigma_2 = A^T P_2 - A_c^T P_2 + P_1 LC_2$,

$\Sigma_3 = A^T P_2 - C_2^T L^T P_2 + P_2 A - P_2 LC_2$.

It is easy to know by the Lyapunov stabilization theory, the system (11) is robust stabilizable with observer-based control (12) when $\dot{V}(\hat{x}(t), e(t)) < 0$. The optimal H_∞ controller is a control law that can minimize the H_∞ norm of the transfer function from disturbance input $w(t)$ to regulated output $z(t)$, namely $min\left(\vartheta = \|T_{wz}(s)\|_\infty\right)$, where ϑ is disturbance attenuation. The H_∞ norm of transfer function $T_{wz}(s)$ can be calculated as:

$$\vartheta = \|T_{wz}(s)\|_\infty = \|z\|_2 / \|w\|_2 = \sqrt{z(t)^T z(t)} / \sqrt{w(t)^T w(t)}$$
$$\Rightarrow z(t)^T z(t) = \vartheta^2 w(t)^T w(t)$$
(16)

Define a cost function by:

$$\hat{J}\left(\hat{x}(t), e(t), w(t)\right) = \dot{V}\left(\hat{x}(t), e(t)\right)$$
$$+ z(t)^T z(t) - \vartheta^2 w^T(t)w(t) \quad (17)$$

Noted that $z(t) = C_1 x(t) + D_1 w(t)$ in system (11), so the Equation (17) can be rewritten as:

$$\hat{J}\big(\hat{x}(t), e(t), w(t)\big) = \begin{bmatrix} \hat{x}(t) \\ e(t) \\ w(t) \end{bmatrix}^T \left\{ \begin{bmatrix} \Sigma_1 & \Sigma_2 & 0 \\ \Sigma_2{}^T & \Sigma_3 & P_2 B_1 \\ 0 & B_1^T P_2 & -\vartheta^2 I \end{bmatrix} \right. $$
$$+ \left. \begin{bmatrix} C_1^T \\ C_1^T \\ D_1^T \end{bmatrix} \begin{bmatrix} C_1^T \\ C_1^T \\ D_1^T \end{bmatrix}^T \right\} \begin{bmatrix} \hat{x}(t) \\ e(t) \\ w(t) \end{bmatrix}$$

(18)

If $\begin{bmatrix} \Sigma_1 & \Sigma_2 & 0 \\ \Sigma_2{}^T & \Sigma_3 & P_2 B_1 \\ 0 & B_1^T P_2 & -\vartheta^2 I \end{bmatrix} + \begin{bmatrix} C_1^T \\ C_1^T \\ D_1^T \end{bmatrix} \begin{bmatrix} C_1^T \\ C_1^T \\ D_1^T \end{bmatrix}^T \leq 0$, it is

easy to know $\dot{V}(\hat{x}(t), e(t), w(t)) \leq 0$ because

$z(t)^T z(t) = \vartheta^2 w(t)^T w(t)$. Define

$\begin{bmatrix} P_1 & 0 & 0 \\ 0 & P_2 & 0 \\ 0 & 0 & I \end{bmatrix} = \begin{bmatrix} X_1^{-1} & 0 & 0 \\ 0 & X_2^{-1} & 0 \\ 0 & 0 & I \end{bmatrix} > 0$ and Pre- and

post-multiply the matrix

$\begin{bmatrix} \Sigma_1 & \Sigma_2 & 0 \\ \Sigma_2{}^T & \Sigma_3 & P_2 B_1 \\ 0 & B_1^T P_2 & -\gamma^2 I \end{bmatrix} + \begin{bmatrix} C_1^T \\ C_1^T \\ D_1^T \end{bmatrix} \begin{bmatrix} C_1^T \\ C_1^T \\ D_1^T \end{bmatrix}^T$, we can have:

$$\Pi = \begin{bmatrix} \Xi_1 & \Xi_2 & 0 \\ \Xi_2{}^T & \Xi_3 & B_1 \\ 0 & B_1^T & -\gamma^2 I \end{bmatrix} + \begin{bmatrix} X_1 C_1^T \\ X_2 C_1^T \\ D_1 \end{bmatrix} \begin{bmatrix} X_1 C_1^T \\ X_2 C_1^T \\ D_1 \end{bmatrix}^T$$

(19)

where， $\Xi_1 = X_1 A_c^T + X_1 K^T B_2^T + A_c X_1 + B_2 K X_1$,

$\Xi_2 = X_1 A^T - X_1 A_c^T + L C_2 X_2$,

$\Xi_3 = X_2 A^T - X_2 C_2^T L^T + A X_2 - L C_2 X_2$.

The controller gain K and the observer gain L in Equation (12) can be calculated by following LMIs optimization problem.

$$\min_{X_1, X_{11}, X_{22}, \hat{A}_c, \hat{K}, \hat{L}} \vartheta \qquad (20)$$

$$s.t. \begin{bmatrix} \Xi_1 & \Xi_2 & 0 & X_1 C_1^T \\ \Xi_2{}^T & \Xi_3 & P_2 B_1 & X_2 C_1^T \\ 0 & B_1^T P_2 & -\vartheta^2 I & D_1^T \\ C_1 X_1 & C_1 X_2 & D_1 & -I \end{bmatrix} < 0 \qquad (21)$$

4. BRAKING FORCE DISTRIBUTION

The direct yaw-moment is calculated by the controller to adjust vehicle attitude. It is to be noted that this moment is added to the center of vehicle gravity but not realized by the braking forces of four wheels. Direct yaw-moment allocation is essentially a constrained optimization problem, by which the direct yaw-moment is reasonably allocated to the braking force of each wheel while the constraints of actuators and the current work status of each wheel are considered. So another important of this paper is how to distribute the braking force at four motored wheel according to the direct yaw-moment.

From Equation (2), it is easy to know that the direct yaw-moment can be expressed by the torque that generated by four tire longitudinal force refer to the center of vehicle gravity. So the realization of direct yaw-moment is to adjust the four longitudinal forces, namely to adjust the braking forces $F_{xi} (i = 1, 2, 3, 4)$. It is necessary to note, however, that for a determined direct yaw-moment M_z , the allocation scheme of $F_{xi} (i = 1, 2, 3, 4)$ is undetermined. The strategy of braking force distribution is to achieve optimal allocation scheme according to an objective function.

One et al [8] allocated the tangential force of the wheels on the ground to minimize tire-road adhesion utilization and retain sufficient adhesion margin for vehicle stable traveling. The road adhesion force of a vehicle can be decomposed into a longitudinal force and a lateral force, and the maximum road adhesion force can be expressed by the product of wheel vertical load and road adhesion coefficient. So the minimization of the tire-road adhesion utilization can be achieved by the solution of the following optimization problem.

The objective function defined as:

$$\min J = \sum_{i=1}^{4} \frac{\sqrt{F_{xi}{}^2 + F_{yi}{}^2}}{\mu F_{zi}} = \sum_{i=1}^{4} \frac{F_i}{\mu F_{zi}} \qquad (22)$$

where, $F_{zi} (i = 1, 2, 3, 4)$ are four wheel vertical load and they can simply expressed as

$$F_{zi} = \frac{mgl_r}{2(l_f + l_r)} \ (i = 1, 2) \ \text{ or } \ F_{zi} = \frac{mgl_f}{2(l_f + l_r)} \ (i = 3, 4);$$

μ is road adhesion coefficient;

$\sqrt{F_{xi}{}^2 + F_{yi}{}^2} \ (i = 1, 2, 3, 4)$ are the road adhesion force which can represented by $F_i \ (i = 1, 2, 3, 4)$.

The constraint conditions defined as:

$$M_z = 0.5t_w \left(F_{x1} - F_{x2} + F_{x3} - F_{x4} \right) \qquad (23)$$

$$F_i = \sqrt{F_{xi}^2 + F_{yi}^2} \leq \min\left(\mu F_{zi}, \left| \frac{T_{max}}{r} \right| \right) \qquad (24)$$

where, T_{max} is the maximum torque of wheel-motor; r is wheel rolling radius.

The above optimization problem can be treated as a linear programming problem and can be expressed as:

$$\begin{array}{ll} \min & f'x \\ sub.\ to: & \begin{cases} Ax \leq b \\ A_{eq}x = b_{eq} \\ lb \leq x \leq ub \end{cases} \end{array} \qquad (25)$$

Where, $f = \dfrac{1}{\mu}\begin{bmatrix} \dfrac{1}{F_{z1}} & \dfrac{1}{F_{z2}} & \dfrac{1}{F_{z3}} & \dfrac{1}{F_{z4}} \end{bmatrix}^T$,

$x = \begin{bmatrix} F_1 & F_2 & F_3 & F_4 \end{bmatrix}^T$, $A = \begin{bmatrix} 1 & 0 & 0 & 0 \\ 0 & 1 & 0 & 0 \\ 0 & 0 & 1 & 0 \\ 0 & 0 & 0 & 1 \end{bmatrix}$,

$b = \dfrac{1}{\mu}\begin{bmatrix} \dfrac{1}{F_{z1}} & \dfrac{1}{F_{z2}} & \dfrac{1}{F_{z3}} & \dfrac{1}{F_{z4}} \end{bmatrix}^T$,

$A_{eq} = 0.5t_w \begin{bmatrix} \cos(\delta+\beta) & -\cos(\delta+\beta) & \cos(\beta) & -\cos(\beta) \end{bmatrix}$,

$b_{eq} = \begin{bmatrix} M_z \end{bmatrix}$, $lb = -\dfrac{T_{max}}{r}\begin{bmatrix} 1 & 1 & 1 & 1 \end{bmatrix}^T$,

$ub = \dfrac{T_{max}}{r}\begin{bmatrix} 1 & 1 & 1 & 1 \end{bmatrix}^T$.

When the linear programming problem is solved, The optimal allocation scheme of the road adhesion forces, F_i $(i=1, 2, 3, 4)$, are obtained, then the four braking forces can be calculated by:

$$F_{xi} = F_i \cos(\delta+\beta) \quad (i=1, 2) \qquad (26)$$

$$F_{xi} = F_i \cos(\beta) \quad (i=3, 4) \qquad (27)$$

5. SIMULATION AND ANALYSIS

In this section, a numerical simulation is conducted to verify the effectiveness of the control system which applied on the 2-DOF vehicle model for handling and stability improvement. The architecture of the observe-based H∞ DYC system proposed in this paper is shown as Figure 2. The primary components of control system includes vehicle dynamic model, desired dynamic response model, side slip observer, optimal H∞ controller and braking force distribution controller. The vehicle

dynamic model is used to compute the yaw rate γ only because the sideslip angle β is immeasurable directly. The direct yaw-moment M_z in Equation (2) is replaced as four braking forces F_{xi} $(i=1, 2, 3, 4)$ which are determined by braking force distribution controller based on direct yaw-moment M_z . The desired dynamic responses of sideslip angle β_d and yaw rate γ_d are output by desired dynamic responses model that defined in Equation (7). It should be noted that the sideslip observer defined in Equation (12) uses the yaw rate γ and the direct yaw-moment M'_z of previous simulation step to estimate sideslip angle $\hat{\beta}$. At last, the optimal H∞ controller calculates the direct yaw-moment M_z for next simulation step.
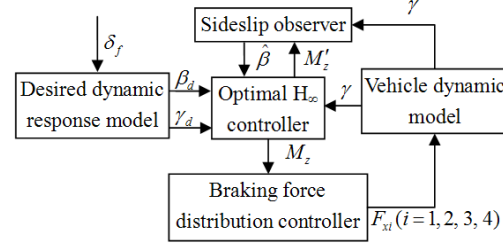

Figure 2: Architecture of the Observe-based H∞ DYC System

The parameters for simulation are: $g = 9.8 \text{m/s}^2$, $m = 1,704.7 \text{ kg}$, $t_w = 1.535 \text{m}$, $l_f = 1.035 \text{ m}$, $l_r = 1.655 \text{ m}$, $C_f = 52,925 \text{ N/rad}$, $C_r = 39,515 \text{ N/rad}$, $r = 0.313 \text{ m}$, $T_{max} = 600 N/m$, $I_z = 3,048 \text{ kgm}^2$. The initial vehicle velocity is 120 km/h, the right and left road surface adhesion are 0.8 and 0.5, respectively. The front-wheel steer angle of a lane change maneuver is defined in Figure 3.

As shown in Figure 4, the direct yaw-moment computed by optimal H∞ controller is allocated to four braking forces. Because the contribution of braking force to direct yaw-moment for front left wheel (front right wheel) and rear left wheel (rear right wheel) is same, as well as the road surface adhesion is same, their braking forces are equal as Figure 4. In the meantime we can see from Figure 4, the braking forces of front left wheel and rear left wheel take a leadership role at 2s to 2.8s and 3.8s to 4s, and the braking forces of front right wheel and rear right wheel take a leadership role at 2.8s to 3.8s. The reasons for this are the braking force distribution controller try to minimize tire-road adhesion utilization and to retain sufficient adhesion

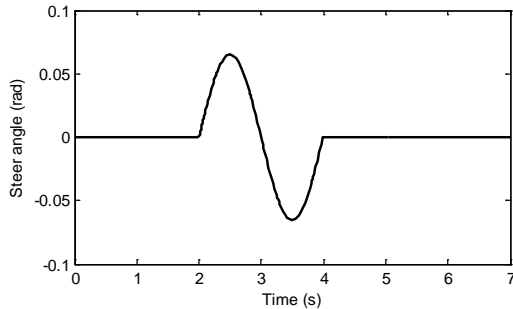margin for vehicle stable traveling, so they work on different time.
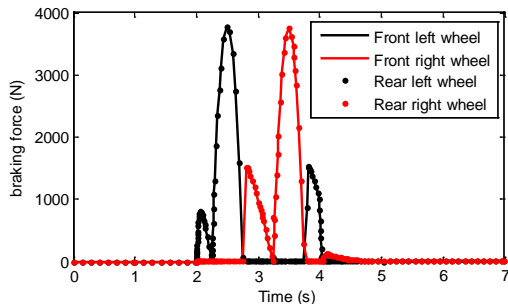

Figure 3: Steering Angle Input in Simulation

Figure 4: Four Braking Forces

The responses of sideslip angle and yaw rate in passive case and active case are compared in Figure 5 and Figure 6, respectively. The two figures show that the sideslip angle and yaw rate can satisfy the desired response when the optimal H_∞ controller is working. The comparative results indicated that the observe-based H_∞ DYC system can improve vehicle handling and stability significantly, and the braking force distribution controller can allocate the direct yaw-moment to four braking forces perfectly.
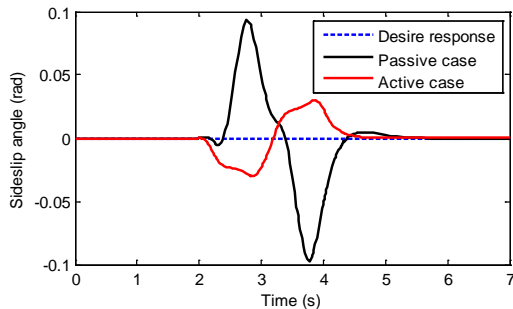

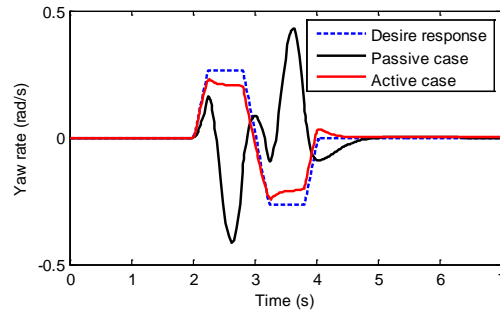
Figure 5: Comparison of Sideslip Angle

Figure 6: Comparison of Yaw Rate

6.   CONCLUSION

A new method of VDC designing and braking force distribution for four wheel in-wheel-motored electric vehicle was introduced. In this paper, the observe-based H_∞ DYC system, which assisted by sideslip angle observer to estimate sideslip angle, is designed to improve vehicle maneuverability and lateral stability. The braking force distribution controller distribute the direct yaw-moment to four braking forces by minimize tire-road adhesion utilization and retain sufficient adhesion margin for vehicle stable traveling. The results of numerical simulation verified that the observe-based H_∞ DYC system can improve vehicle handling and stability significantly and the braking force distribution controller can consider the constraints of actuators and the current work status of each wheel fully.

ACKNOWLEDGEMENTS

REFRENCES:

[1] M. Akar, and J.C. Kalkkuhl, "Lateral dynamics emulation via a four-wheel steering vehicle", *Vehicle System Dynamics*, Vol. 46, No. 9, 2008, pp. 803-829.

[2] X. Yang, Z. Wang, and W. Peng, "Coordinated control of AFS and DYC for vehicle handling and stability based on optimal guaranteed cost theory", *Vehicle System Dynamics*, Vol. 47, No. 1, 2009, pp.57-79.

[3] C. Geng, L. Mostefai, M. Denaï, and Y. Hori, "Direct yaw-moment control of an in-wheel-motored electric vehicle based on body slip angle fuzzy observer", *IEEE Transactions on Industrial Electronics*, Vol. 56, No. 5, 2009, pp.1411-1419.

[4] J. Wang, Q. Wang, L. Jin, and C. Song, "Independent wheel torque control of 4WD electric vehicle for differential drive assisted steering", *Mechatronics*, Vol. 21, No. 1, 2011, pp.63-76.

[5] B.L. Boada, M.J.L. Boada, and V. Díaz, "Fuzzy-logic applied to yaw moment control for vehicle stability", *Vehicle System Dynamics*, Vol. 43, No. 10, 2005, pp.753-770.

[6] C.J. Kim, J.H. Jang, S.K. Oh, J.Y. Lee, C.S. Han, and J.K. Hedrick, "Development of a control algorithm for a rack-actuating steer-by-wire system using road information feedback", *Proc. IMechE, Part D: Journal of Automobile Engineering*, Vol. 222, No. 9, 2008, pp.1559-1571.

[7] R. Rajamani, "Vehicle Dynamics and Control", Springer, New York, 2006.

[8] E. Ono, and Y. Hattor, "Vehicle dynamics integrated control for four-wheel-distributed steering and four-wheel-distributed traction/ braking system", *Vehicle System Dynamics*, Vol. 44, No. 2, 2006, pp.139-151.